Parameter Sensitivity of the Noah-MP Land Surface Model with Dynamic Vegetation

Kristi R. Arsenault[*,1,2]*; Grey S. Nearing*[3]*; Shugong Wang*[1,2]*; Soni Yatheendradas*[1,4]*; Christa D. Peters-Lidard*[5]

[*]*Corresponding Author: 8800 Greenbelt Rd; Greenbelt, MD 20771; Code 617, Bldg 33; (301)-614-5772; kristi.r.arsenault@nasa.gov*
[1]*NASA GSFC, Hydrological Sciences Laboratory; Greenbelt, MD 20771*
[2]*Science Applications International Corporation; McLean, VA 22102*
[3]*University of Alabama Department of Geological Sciences; Tuscaloosa, AL 35487*
[4]*University of Maryland, Earth Science Interdisciplinary Center; College Park, MD 20704*
[5]*Earth Sciences Division, NASA Goddard Space Flight Center, Greenbelt, MD*

Abstract

The Noah land surface model with multiple parameterization options (Noah-MP) includes a routine for dynamic simulation of vegetation carbon assimilation and soil carbon decomposition processes. To use remote sensing observations of vegetation to constrain simulations from this model, it is necessary first to understand the sensitivity of the model to its parameters. This is required for efficient parameter estimation, which is both a valuable way to use observations and also a first or concurrent step in many state-updating data assimilation procedures. We use variance decomposition to assess the sensitivity of estimates of sensible heat, latent heat, soil moisture, and net ecosystem exchange made by certain standard Noah-MP configurations that include dynamic simulation of vegetation and carbon to forty-three primary user-specified parameters. This is done using thirty-two years' worth of data from ten international FluxNet sites. Findings indicate that there are five soil parameters and six (or more) vegetation parameters (depending on the model configuration) that act as primary controls on these states and fluxes.

1. Introduction

Globally, transpiration accounts for more than four-fifths of the total evaporative flux (Jasechko et al., 2013), and thus vegetation plays a key role in coupling the water and energy balances at the land surface with the atmosphere. At present, many operational land data assimilation systems (LDASs) do not dynamically simulate vegetation, and instead rely on prescribed vegetation indices (*e.g.*, Ek et al., 2003, Chen and Dudhia, 2001, Xia et al., 2011, Case et al., 2011, Rodell et al., 2004, Hao et al., 2014). This limits the ability of these systems to assimilate different types of vegetation data products.

If LDASs were instead to use land surface models (LSMs) that directly simulate plant carbon uptake and partitioning, then vegetation-related observations could be assimilated directly, and these LDAS frameworks would be able, at least in theory, to derive information from almost any vegetation remote sensing product. Recently, the Noah LSM (Ek et al., 2003) was extended into a multi-physics simulation platform (Noah-MP) that includes a dynamic vegetation component (Niu et al., 2011). This model has the potential to facilitate assimilation of remote sensing vegetation products and indices into terrestrial hydrologic forecast and monitoring systems (*e.g.*, Ek et al., 2003, Xia et al., 2011, Case et al., 2011).

Currently, there are a plethora of high-quality vegetation-monitoring products available from various remote-sensing platforms (*e.g.*, Running et al., 2004, Jiang et al., 2008, Dash and Curran, 2004, Didan and Huete, 2006, Huete, 1988, Deng et al., 2006, Vogelmann et al., 2001, Zhu et al., 2013) that could, in principle, be used to constrain or otherwise inform these large-scale LDAS or other hydrologic forecast systems. The two most important methods in terrestrial hydrology for constraining model simulations with observations are parameter estimation (*e.g.*, Rosolem et al., 2013) and state-updating data assimilation (*e.g.*, Reichle, 2008). Related to the latter, by far the most common algorithms (*e.g.*, Evensen and van Leeuwen, 2000) are bias-blind (Dee, 2005). As such, they require that the observations

and the model predictions have identical climatology – that is, bias-blind algorithms are not effective at estimating systematic differences in the mean state of the model as compared to that of observations. It cannot be expected that any parameterized model and any set of indirect remote sensing observations, which are themselves typically dependent on a parameterized retrieval model, will have mutually consistent climatologies (*e.g.*, Reichle and Koster, 2004). It is necessary, therefore, to somehow map the observations to the model climatology or vice versa. The two primary methods for doing this are (1) via parameter estimation or (2) via non-parametric regression – *i.e.*, matching of cumulative density functions (e.g., Kumar et al., 2012). The density matching approach is inefficient in the sense that it discards potentially valuable information (*e.g.*, Kumar et al., 2015), and therefore parameter estimation is (or should be) an important part of robust methods for combining information from models and remote sensing data.

Parameter estimation is extremely computationally expensive, with costs that rise – typically – closer to exponentially than linearly in the number of parameters, and an important first step is to reduce the number of parameters to be estimated via sensitivity analysis. Many sensitivity analyses have been performed on the various models that underlie most of the major land data assimilation systems (*e.g.*, Demaria et al., 2007, Xue et al., 1996, Chen and Dudhia, 2001, Pitman, 1994, Hou et al., 2012, Liang et al., 1996, Bastidas et al., 1999), including the Noah model (Rosero et al., 2010, Hogue et al., 2005, Hogue et al., 2006, Hou et al., 2015), and Noah-MP in particular (Cai et al., 2014a; Mendoza et al., 2015; Cuntz et al., 2016). Cuntz et al., (2016) performed a sensitivity analysis with Noah-MP, focusing on hydrological variables such as latent heat flux and runoff components, at catchment scales. However, none of these studies have looked at the sensitivity of parameters specifically related to the dynamic vegetation.

Our purpose here is very specific: to assess the sensitivity of the model to its parameters in a way that is general enough to provide guidance on parameter estimation either as a stand-alone method or pre-

requisite for assimilating vegetation-related remote sensing products into land data assimilation type systems. Our strategy is to assess the sensitivity of LSM estimates of the major hydrologic states and fluxes to variations in prescribed parameter values. Sensitivity analysis is an investigation of the model equations and parameters, not an investigation of the model's ability to reproduce observations, nor is it an investigation of the value of any particular set of observations for informing the model simulation. As such, high-quality in situ observations of storage states (soil moisture) and fluxes (sensitive and latent heat, and net ecosystem exchange), like what are available from the FluxNet observing network, are preferable to satellite-based observations for this task – even though it is satellite-based observations that will ultimately be used by LDAS systems. Energy fluxes, like latent heat flux, are important for land-atmosphere interactive processes, especially in weather forecasting and climate models. Also, soil moisture is a critical variable used in determining agricultural drought, water and food security, etc., and the net carbon or ecosystem exchange is important to better understanding and modeling CO_2 fluxes regionally and globally.

The following section describes the model, forcing data, observation data, and methodology used in this study. Section 3 presents the primary results of our analysis. The objective of this paper is to serve as a concise resource for directing parameter estimation with the dynamic vegetation component of Noah-MP, and as such, we have made every effort to keep this report short and to the point, with the main results easily accessible.

2. Data and Methods

2.1. FluxNet Observations

Observations used for this experiment, both as meteorological forcing data to run the model and as response data against which to calculate sensitivity indices, were taken from ten of the FluxNet (Baldocchi et al., 2001; *fluxnet.ornl.gov*) sites included in the Protocol for Analysis of Land Surface

Models (PALS; Abramowitz, 2012). These sites were used, for example, by Best et al. (2015) to evaluate and compare performance of most of the land surface models referenced in the introduction. The subset of PALS sites used here included all of the landcover types in the original PALS data set except for broadleaf forests (the subset does include a mixed forest site, Sylvania, which is a deciduous forest) and permanent wetlands. We employed a total of thirty-two years' worth of data, as outlined in Table 1. These data-years were chosen from the complete collection of PALS level-4 (gap-filled) FluxNet data on the criteria that they include half-hourly measurements of sensible heat, Q_h [W/m^2], latent heat, Q_{le} [W/m^2], net ecosystem exchange, NEE [μmol/m^{2}s], and soil moisture [m^3/m^3] measured at two different depths, θ_1 and θ_2 (the soil moisture measurement depths vary by site and are listed in Table 1). These data were then used to estimate model sensitivity via a function of the residuals between model predictions and FluxNet observations as described in section 2.4.

Forcing data included 2-meter air temperature [K], rainfall rate [mm/s], relative humidity [kg/kg], wind speed [m/s], surface pressure [hPa], incident longwave radiation [W/m^2], and incident shortwave radiation [W/m^2]. These data were recorded from each FluxNet site at 30 minute intervals, and the model configurations were run on the same 30 minute timestep. The model runs were initialized according to PALS protocol: by running the model using a forcing data record that includes all of the available data at a particular site repeated ten times in sequence. Each model was initialized at each site in this manner exactly once using a default set of parameters, and an initial state was captured at the beginning of each simulation year listed in Table 1. Repeating the spin-up for each model separately for all of the requisite sensitivity runs would require on the order of hundreds of thousands of processor-hours, and is therefore infeasible. The default spin-up parameters were extracted via STATSGO-FAO soil data (Miller and White, 1998) and the U.S. Geological Survey (USGS) vegetation classification maps (Anderson, 1976, Pielke et al., 1997, Chen and Dudhia, 2001) and utilized by the standard Noah-MP look-up tables.

2.2. Model

Noah-MP (Niu et al., 2011; Yang et al., 2011) expands upon the Noah LSM (Ek et al., 2003). Noah is an important component of many (especially U.S.-based) land data assimilation systems because it is coupled with the Weather Research and Forecast (WRF) model and is used operationally by the US National Center for Environmental Prediction (NCEP) and U.S. Air Force 557th Weather Squadron.

Noah-MP includes options for parameterizing ten distinct land surface states and processes; these are listed in Table 2. Three of these options (first three lines in Table 2) are related to vegetation; these are: (1) the parameterization of leaf area index and vegetation shade fraction, (2) the stomatal resistance parameterization, and (3) the effect of soil moisture on stomatal resistance. In total, there are 1728 possible Noah-MP configurations with dynamic vegetation, and it is impossible to assess parameter sensitivity under all of these configurations. To reduce the number of configurations, we note that the Noah-MP has a "default" configuration outlined in the public release code, and we used the default configuration options for all of the non-vegetation related components. This includes seven default options (outlined in column 3 of Table 2); those related to: runoff and groundwater, surface layer drag coefficient, super-cooled liquid water in the soil, frozen soil permeability, radiation transfer, snow albedo, and frozen precipitation partitioning.

Using these seven default options cuts the number of dynamic vegetation configurations to three – dynamic vegetation requires the Ball-Berry stomatal resistance option, and then there are three different parameterizations of soil moisture control on stomatal resistance, β, based on 1) Noah LSM's version, 2) the Community Land Model (CLM), and 3) Simplified Simple Biosphere (SSiB) model equations (Niu et al., 2011), as outlined in Table 2. The Noah LSM version of β is simply a function of soil moisture and wilting point and reference soil moisture parameters, which depend on soil type (Chen et al., 1996), whereas the CLM and SSiB type approaches rely on the matric potential of each soil layer, including the

saturated and wilting matric potential (see Oleson et al., 2010, for CLM, and Xue et al., 1991, for SSiB). Because our purpose here is to test parameter sensitivity related to dynamic vegetation, we explore several model configurations related to two of the three sets of options. Therefore, we compared parameter sensitivity under the three Noah-MP configurations that include dynamic vegetation, and which vary with the soil moisture factor for stomatal resistance (Noah-type, CLM-type, and SSiB-type) against the default Noah-MP configuration, which does not include dynamic vegetation and uses prescribed leaf area index (LAI) and the default (Noah-type) soil moisture factor for stomatal resistance. Thus, in total we compare four Noah-MP configurations. It is important to point out that the options used in the prescribed LAI configuration differ from the parameters used in the dynamic vegetation configurations and also that this default configuration does not simulate net ecosystem exchange. All configurations of Noah-MP were run using four soil layers with thicknesses of 10 cm, 30 cm, 60 cm, and 100 cm (for a total 2 meter profile).

2.3. Parameters

A total of 42 user-specified parameters must be set for the Noah-MP configurations that simulate dynamic vegetation; these are listed in Table 3. Thirty of these parameters are related to vegetation and twelve are related to soil. Similarly, we considered a total of 31 parameters for the Noah-MP configuration that used prescribed LAI. Nineteen of these are related to vegetation and the same twelve (as in the dynamic vegetation configurations) are related to soil; these are listed in Table 4. Aside from the soil parameters, twelve of the vegetation parameters are shared between the two configurations – these are related to the two-stream radiation transfer component. The deep soil temperature parameters (ZBOT and TBOT) are used for the SIMGM runoff and groundwater option that we used in all configurations.

The typical way to assign values to all of these parameters is via look-up tables indexed by USGS vegetation and STATSGO-FAO soil categorization schemes, which is how we derived the default parameters for model spin-up. With a few exceptions, the ranges over which we conducted the sensitivity

159 analysis were bounded by the minimum and maximum values from the Noah-MP look-up tables; Tables
160 3 and 4 list these ranges. The exceptions are as follows. LAI and SAI (stem area index) are prescribed to
161 the model as monthly values, so in reality there are 24 LAI and SAI parameters. We assessed the general
162 influence of LAI and SAI by measuring sensitivity to a multiplier that scaled the entire LAI (SAI) time
163 series. Additionally, the four soil moisture parameters that are expressed as volumetric water contents
164 (porosity, wilting point, field capacity, and dry soil) were constrained to preserve an appropriate ordering
165 relationship (*i.e.*, field capacity must be lower than porosity, wilting point lower than field capacity, and
166 dry soil lower than wilting point). Porosity was allowed to vary between hard limits (listed in the parameter
167 tables), and instead of assigning ranges to the other three volumetric water content parameters directly,
168 we assessed sensitivity to hyperparameters that represented the percentage of the difference between the
169 lower bound listed in Tables 3 and 4 and the parameterized upper limit according to the ordering
170 relationship mentioned above. Finally, we lowered the range of the single-side leaf area (SLA) parameter,
171 which is vegetation type dependent, since previous studies, which Noah-MP is somewhat based on,
172 included lower SLA values (e.g., Dickinson et al., 1998; Gulden and Yang, 2006).

173 **2.4. Sensitivity Analysis**

174 A variance-based global sensitivity analysis was applied to the four chosen Noah-MP
175 configurations to derive total sensitivity indices for each of the parameters listed in Tables 3 and 4 and
176 related to each of the five different observed responses: $Q_h, Q_{le}, NEE, \theta_1,$ and θ_2. In the following
177 equations, the parameters are notated such that x_i is the i^{th} (of N) parameter, and $\boldsymbol{x}_{\sim i}$ is a vector of the
178 other $N-1$ parameters. The total effect index associated with (scalar) x_i is (Saltelli et al., 2009, page
179 178):

$$T_i = 1 - \frac{E_{x_i}[f(\boldsymbol{x}_{\sim i}, x_i)^2] - E_x[f(\boldsymbol{x})]^2}{E_x[f(\boldsymbol{x})^2] - E_x[f(\boldsymbol{x})]^2} \quad [1]$$

Monte Carlo approximation of the integrals over M samples yields:

$$E_x[f(\boldsymbol{x})] = \sum_{m=1}^{M} f(\boldsymbol{x}_m) \quad [2.1]$$

$$E_x[f(\boldsymbol{x})^2] = \sum_{m=1}^{M} f^2(\boldsymbol{x}_m) \quad [2.2]$$

$$E_{x_i}[f(\boldsymbol{x}_{\sim i}, x_i)^2] = \sum_{m=1}^{M} f\left(\boldsymbol{x}_{\sim i}^{(1)}, x_i^{(1)}\right) f\left(\boldsymbol{x}_{\sim i}^{(1)}, x_i^{(2)}\right) \quad [2.3]$$

The final integral requires two sets of M samples, so that $x_{i,m}^{(1)}$ is drawn from one $\boldsymbol{X}^{(1)} \in \mathbb{R}^{N,M}$ and $x_{i,m}^{(2)}$ is drawn from one $\boldsymbol{X}^{(2)} \in \mathbb{R}^{N,M}$. $\boldsymbol{X}^{(1)}$ and $\boldsymbol{X}^{(2)}$ were drawn by Latin hypercube sampling with $M = 1500$ (an investigation of the effect of sample size is presented as supplementary material). In this case, the f function is the mean-squared error between the model predictions and FluxNet observations.

Total effect indices were calculated separately for each observation type (e.g., latent heat flux, soil moisture) and for each data year. This allowed us to have some idea of the inter-annual variability in sensitivity depending on different climatic conditions, and also of the variability in sensitivity relative to different biomes present at different sites. It is important to point out that the soil moisture measurements at each site were at different depths (see Table 1), and so each measurement was compared with the soil moisture content of the confining model layer (see section 2.2). In the case where soil moisture observations were at a layer boundary (*e.g.*, the 10 cm measurements at Blodgett, Mopane, and Sylvania), we used the average of the modeled moisture content in the two layers. This worked at every site except

Hyytiala, where both soil moisture measurements were in the 2-3 cm to 5 cm of the soil column, which did affect results, as described in section 3.1.

3. Results

Figures 1 to 5 present results from a total of 608 sensitivity analyses (five observed variables over 32 data-years using three configurations with dynamic vegetation, plus four observed variables over 32 years using the default configuration without dynamic vegetation). Each figure presents results for a different model output ($Q_h, Q_{le}, NEE, \theta_1, \theta_2$). The different subplots in each figure represent the different model configurations (i.e., three different stomatal resistance functions, plus prescribed vegetation). The mean total sensitivity index averaged over all years at each site is reported in each figure (grouped by color and symbol), as well as the fraction of variance in the sensitivity indices for each parameter and model configuration that is explained by differences between sites (this fraction of explained variance is called "EV" and represented by gray bars in the figures). The remaining unexplained fraction of variance is due differences between years at individual site – this was calculated as a straightforward application of the law of total variance. The site and year variance decompositions were calculated for any parameter with at least one site-year with $T_i > 0.1$.

3.1. Dynamic Vegetation Results

The results from the CLM-type and SSiB-type soil moisture resistance factor configurations were essentially qualitatively identical in all output variables. Further, certain parameters displayed clear sensitivity over most observed variables (Figures 1-5) and in all three dynamic vegetation configurations (CLM-type, SSiB-type, and Noah-type). These included four vegetation parameters: QE25 (baseline light-use efficiency), VCMX25 (baseline maximum rate of carboxylation), LTOVRC (leaf turnover rate) and SLA (single-side leaf area per kg), as well as two soil parameters: SMCWLT (wilting point) and BEXP (pore size distribution index). The two soil parameters control direct soil evaporation, soil conductivity

and diffusivity, and stomatal resistance in the CLM-type and SSiB-type configurations, and therefore act as direct controls on both soil moisture content and surface energy partitioning through the evaporative flux. QE25 and VCMX25 directly control light-limited and export-limited photosynthesis respectively (the export limit is mediated by local air pressure), and LTOVRC controls carbon exchange from plant to soil due to leaf and stem senescence. SLA is dependent on vegetation type and used in determining the leaf and stem area index. We would classify these six parameters as the most important user-specified parameters in the model (see also Mendoza et al., 2015). Also, the observed soil moisture variables (Figures 3 and 4) have higher sensitivities to the SMCREF, SMCMAX, and DKSAT soil parameters for all three soil moisture stomatal resistance parameterizations, and to a lesser extent for fluxes Q_{le} (Figure 1), Q_h (Figure 2), and NEE (Figure 5), for the Noah-type parameterization only. Cuntz et al. (2016) found SMCMAX (soil porosity) to be the most sensitive parameter across different fluxes and catchment areas, and to a lesser extent the SMCREF parameter, when transpiration is controlled more by soil moisture limitations. In comparison to our study, they used the prescribed monthly LAI with constant shade fraction (option 4), the Ball-Berry (option 1) for stomatal resistance, and the Noah configuration for soil moisture factor for stomatal resistance.

The surface fluxes Q_{le} and Q_h at two sites - grassland (Fort Peck) and deciduous forest (Sylvania) -- exhibited some sensitivity to Z0MVT (momentum roughness length) and to HVT (canopy height) in the different model configurations (Figures 1 and 2). Roughness length controls surface advection potential, and the 3-D vegetation model in the radiation transfer scheme uses canopy height to compute total available energy at the soil and vegetation surfaces. Varying these controls has the greatest effect in the shortest (grassland) and tallest (deciduous forest) canopies. High sensitivity to HVT was also reported in Cuntz et al. (2016) for evapotranspiration. It is additionally interesting to note the high sensitivity of NEE (Figure 5) at Fort Peck and Amplero grassland sites, and to some extent the Krueger savanna site, to

239 the canopy height and roughness length parameters for net ecosystem exchange. Growing unrealistically
240 tall grass causes a large divergence in the modeled carbon flux, and these parameters would be a large
241 source of error in mis-specified grasslands.

242 In the Noah-type configuration, SMCREF (field capacity) exerts a control on calculating plant
243 water stress, and in the CLM-type and SSiB-type configurations, BEXP dominates the water stress
244 calculation by acting as an exponential factor in the stomatal resistance calculation. Plant water stress
245 determines both the amount of water available for transpiration (*i.e.*, acts as a control on surface energy
246 partitioning and root zone water uptake) and also total carbon assimilation. The result is that field capacity
247 is an important parameter for determining all five states and fluxes in the Noah-type configuration, which
248 was also shown in Cuntz et al. (2016) for transpiration. In the CLM- and SSiB-type configurations, all
249 five states and fluxes are more sensitive to pore size distribution index (BEXP) than in the Noah-type
250 configuration. For the Noah-type configuration, the surface fluxes (Figures 1 and 2) were only marginally
251 sensitive to BEXP and slightly more so with SMCDRY, especially at the savanna sites (Mopane and
252 Krueger), which are both in semi-arid areas (Hanan et al., 2011, Veenendaal et al., 2004). Similarly at the
253 Mopane and Kruger sites, and also at the El Saler 2 agricultural site, soil moisture, especially at the shallow
254 measurement depth, was sensitive to certain plant-related parameters that determine vegetation
255 productivity: light-use efficiency (QE25) and carboxylation (VCMX25). These two vegetation
256 parameters are mainly tied to Noah-MP's photosynthesis processes, based on a modified version of
257 Farquhar et al. (1980) C3 plant model (Collatz et al., 1991). Also for the same reason, the surface energy
258 balances (Q_{le} and Q_h; Figures 1 and 2) at these water-limited sites were sensitive to PSISAT (saturated
259 matric potential) in the CLM- and SSiB-type configurations. PSISAT is not used in the Noah-type
260 configuration – it is used as a linear function (rather than exponential, like BEXP) in the CLM- and SSiB-

type calculations of stomatal resistance. These semi-arid sites are also much more sensitive to the pore size distribution index in the CLM-type and SSiB-type configurations than the other sites.

In addition to the two universally sensitive soil parameters (wilting point and unsaturated conductivity exponent), soil moisture (Figures 3 and 4) was also sensitive to SMCMAX (porosity) and DKSAT (saturated hydraulic conductivity) in all model configurations, and SMCREF in the top soil moisture layer (Figure 3). In most land surface models, porosity is a dominant control on soil moisture (and here also on plant water availability and stress), since porosity influences both diffusion and advection in the soil, as well as total water holding capacity. Saturated conductivity is the primary influence on moisture transport between soil layers.

Carbon flux (net ecosystem exchange; Figure 5) is a sum of plant carbon assimilation, plant respiration and soil respiration, and so it is sensitive to essentially the same set of factors as the surface energy balance terms and soil moisture states. The only additional parameter that showed sensitivity here (in all configurations) was RMF25 (leaf maintenance respiration). This parameter represents a baseline respiration rate that is modified by factors related to plant water stress, energy availability, and air temperature. Water stress and energy availability are the two main controls discussed that mediate the relationship between model parameters and the model-predicted surface energy balance and moisture states, and the baseline maintenance respiration is the parameter that translates these factors into estimates of actual plant respiration.

3.2. Prescribed LAI Results

The prescribed LAI simulations required a different parameter set than the dynamic vegetation simulations, although some of the parameters (soil parameters and those related to radiation transfer) are shared with the dynamic vegetation configurations as described above. In this case, however, there was clear sensitivity of sensible heat to several of the reflectance parameters – especially to the leaf reflectance

parameter in the near infrared wavelengths (RHOL-nir). For this configuration, Cuntz et al. (2016) found sensible heat flux to be more sensitive to radiation parameters (RHOS and RHOL) and leaf optical properties (e.g., TAUL). Again, there was clear sensitivity in the surface energy fluxes to Z0MVT (momentum roughness length), and to a lesser degree for the soil moisture observations, mainly at the Fort Peck grassland site for the second level soil moisture. The Sylvania mixed deciduous forest site showed sensitivities for Z0MVT and HVT (canopy height), for the energy fluxes only.

Further, the surface energy fluxes showed sensitivity to most of the vegetation parameters that are specific to this prescribed LAI configuration, except height of bottom of canopy (HVB), tree crown radius (RC), and maximum stomatal resistance (RSMAX). RSMAX controls the portion of canopy resistance due to incoming radiation, whereas TOPT (optimum transpiration) and HS (vapor pressure deficit) control the portion of canopy resistance due to air temperature and vapor pressure deficit, respectively. Both of the latter were more influential on the energy partitioning. Both the LAI and SAI multipliers also contributed substantially to the surface energy balance due to their role in determining total available energy at the surface (also noted similarly for LAI in Cuntz et al., 2016).

In general, there was feedback from the soil state to the energy balance at the surface in this configuration, but much less feedback from the vegetation to the soil moisture state than in the dynamic vegetation configuration. Almost none of the vegetation parameters were important in determining soil moisture states. Generally, the same soil parameters were important in this configuration as in the dynamic vegetation configuration. Wilting point was important for energy partitioning due to its control on water that is available for transpiration. Porosity, field capacity, saturated hydraulic conductivity, and the infiltration exponent dominated the soil moisture sensitivity, which is a standard result in land surface models (e.g., Cuntz et al., 2016).

3.3. Space vs. Time Dependence

To get some idea of how the calculated T_i values are sensitive to intra-site vs. inter-annual differences, we calculated the fraction of variance over the 32 site-years for each parameter of each model configuration. Figures 1 to 5 report the fractions of variance due to intra-site differences for every parameter with at least one site-year of $T_i > 0.1$. In most cases, greater than 80% of the total variance among the 32 site-years is due to different sensitivities at different sites; however, there are a few notable exceptions.

In the Q_e and θ_2 results, the BEXP and SMCWLT parameters (and SMCREF in the static vegetation configuration) show >20% dependency on inter-annual differences between forcing data. These parameters are the primary controls on plant water uptake, and these differences are dominated by dry years at the two semi-arid sites. We did not see the same dependency on forcing data in the surface soil moisture at these two sites because plant water uptake processes do not act as the dominant control on evaporative flux in the surface layer – this is controlled by both root-water uptake and direct evaporation. Inter-annual forcing differences had a larger effect on certain parameter sensitivities related to NEE than to the other modeled variables. In particular, the Amplero grassland site was highly sensitive to the HVB and RC canopy parameters and to the TAUL and TAUS leaf and stem transmittance parameters on two of the three years (2003 and 2006, but not 2004). All of these parameters directly control photosynthesis. We also see selective sensitivity (dependent on forcing) to plant (FRAGR, RMF25) and microbe (MPR) respiration parameters, especially at the water-limited sites.

The main take-away from these results is that the functional response of the carbon cycle components of the dynamic vegetation model(s) is more sensitive to boundary conditions than are the soil-water and energy partitioning components. Ruddell et al. (2016) makes a distinction between the *macrostate* and the *microstate* of a complex dynamical system, where the *macrostate* is the current (but time/space dependent) network and strengths of dynamic process interconnections between different

variables in the model or system (i.e., the model's effective internal functional response surfaces at any given point in time), whereas the *microstate* is the current value of the different variables in the dynamical system or model. Ruddell et al. (2016) show how to measure the dynamic influence of nonstationary boundary conditions on determining a system's macrostate. Here we see a similar phenomenon – Noah-MP can be thought of as a dynamical system with a macrostate (i.e., strength of relationships between different simulated variables within the model) determined by the particular parameter values, and we see that the meteorological data has some impact on the sensitivity of model output to the effective macrostate. In particular, this sensitivity is more pronounced in the dynamic vegetation and carbon cycle components of the model than it is in the traditional hydrology (water and energy) components. We see clearly here that different aspects of the model structure become important for carbon flux simulation depending on differences in forcing data at individual sites. This indicates that it could be significantly more complicated to calibrate a land surface model with dynamic vegetation than one without.

4. Conclusions

To summarize, in the Noah-MP dynamic vegetation configurations, all outputs (surface heat fluxes, soil moisture, and net carbon flux) exhibited sensitivity to the (i) wilting point, (ii) unsaturated soil conductivity exponent, (iii) baseline light-use efficiency, (iv) baseline carboxylation, (v) leaf turnover, and (vi) single-sided leaf area. The surface fluxes are also especially sensitive to (vii) the momentum roughness length, water stress, which is determined either by (viii) field capacity or the conductivity exponent depending on the model configuration, and also in some cases to (ix) canopy height. Soil moisture was sensitive as well to (x) porosity and (xi) saturated soil hydraulic conductivity. Finally, the carbon flux was additionally sensitive to (xii) leaf maintenance respiration. These twelve primary parameters are highlighted in table 3.

The major difference between the dynamic vegetation configurations and the prescribed LAI configuration was that the dynamic vegetation configurations exhibited greater control from vegetation on soil moisture states – that is, dynamic vegetation increased the sensitivity of soil moisture to vegetation parameters. This supports one of the primary conclusions by Yang et al. (2011) that using a land surface model with a dynamic vegetation component may be beneficial to soil moisture modeling (*e.g.*, NWP initial conditions, drought monitoring, etc.). In particular, these sensitivity results show that simulating photosynthesis (*e.g.*, carboxylation and quantum efficiency, carbon leaf stress, leaf turnover) does have the potential to affect couplings between carbon and water processes at the land surface. This suggests that (correctly) parameterizing photosynthesis has the potential to add realism to land model simulations. By identifying key parameters which Noah-MP soil moisture and energy fluxes are most sensitive to, we can better target and modify these for future data assimilation studies, which could include satellite-based vegetation indices (e.g., NDVI, LAI) and higher resolution soils databases. Since Noah-MP is planned to be the main model used by the U.S. National Water Center and currently used by the WRF community, knowing which parameters can affect land-atmospheric interaction, like the energy fluxes, and hydrological forecasts, like soil moisture, can save users much time. As shown in this study, there are dozens of parameters just for these couple of vegetation and soil schemes and thousands of combinations between the options.

It is important to note that we only considered here parameters that the Noah-MP model developers have specified as to be defined by the user. There are several potentially important parameters that are hard-coded into the model, and this hard-coding has the potential to reduce the flexibility of the model in reproducing surface states and fluxes (Mendoza et al., 2015, Cuntz et al., 2016). It is also important to understand that an empirical sensitivity analysis, like what we have presented here, has the potential to miss certain thresholds that may not be activated with the data used for testing. We did see evidence of

this type of threshold behavior in the fact that certain site-years were water-limited in a way that affected plant stress, senescence, and ultimately parameter sensitivity. However, in general, the results were relatively consistent across sites and between the various model configurations. This study should be robust enough to provide general guidance on how to approach parameter estimation for simulation of dynamic vegetation using the Noah-MP LSM.

That being said, there are a combinatorial number of possible Noah-MP configurations (see Table 2), and each configuration at least has the potential for different parameter sensitivities. As such, the data and code used in this study is available publically on GitHub (*https://github.com/greyNearing/NoahMP-Sensitivity.git*), so that anyone interested in running a Sobol' analysis using this set of FluxNet data can do so with their own Noah-MP configuration(s). Re-running this analysis for a different configuration is relatively simple using this code base (written mostly in MatLab). The problem of sampling the parameter space for calculating Sobol' indices is mostly a parallel problem, and our code is set up to run across multiple, distributed memory nodes using a SLURM scheduler. It can also be run on a single processor or single shared-memory node.

Finally, the global variance-based method we used here (Section 2.4) is not the only option for conducting sensitivity analyses. This has become a routine component of model-based hydrological forecasting, data assimilation, and hypothesis testing (Razavi and Gupta, 2015), with many proposed methodologies. In particular, if we were to consider larger parameter spaces (e.g., Mendoza et al., 2015, Cuntz et al., 2015), it may be necessary to use more computationally frugal sensitivity analyses (e.g., Herman et al., 2013, Cuntz et al., 2015, Rakovec et al., 2014). Alternatively, we are sometimes interested in more specific questions related to model parameterization – for example, unlike the analysis presented here, which looked at global model sensitivity with respect to a variety of site-specific ground truth data, a more specific modeling problem (i.e., to a specific site or watershed) might come with a more

constrained parameter uncertainty distribution. In this case, we might want to use a more localized or subspace sensitivity analysis (e.g., Rakovec et al., 2014).

Acknowledgements

This work used data acquired by the FluxNet community and in particular by the following organizations: CarboEuropeIP, CarboItaly and CarboMont (Amplero), AmeriFlux (Blodgett; Goldstein et al., 2000), CarboEuropeIP (El Saler, El Saler 2), AmeriFlux (Fort Peck), University of Helsinki (Hyytiala; Suni et al., 2003), NASA and NSF through grants to Niall Hanan (Kruger; Hanan et al., 2011), ALTERRA, Wageningen UR, and CarboEuropeIP (Loobos; Elbers et al., 2011), CarboAfrica (Mopane; Veenendaal et al., 2004), ChEAS and AmeriFlux (Sylvania; Desai et al., 2005). Computing resources were provided by the NASA Center for Climate Simulation at the NASA Goddard Space Flight Center.

References

Abramowitz, G. (2012) 'Towards a public, standardized, diagnostic benchmarking system for land surface models', *Geoscientific Model Development Discussions*, 5(1), pp. 549-570.

Anderson, J. R. (1976) *A land use and land cover classification system for use with remote sensor data.* US Government Printing Office.

Baldocchi, D., Falge, E., Gu, L., Olson, R., Hollinger, D., Running, S., Anthoni, P., Bernhofer, C., Davis, K. and Evans, R. (2001) 'FLUXNET: A new tool to study the temporal and spatial variability of ecosystem-scale carbon dioxide, water vapor, and energy flux densities', *Bulletin of the American Meteorological Society*, 82(11), pp. 2415-2434.

Ball, J. T., Woodrow, I. E. and Berry, J. A. (1987) 'A model predicting stomatal conductance and its contribution to the control of photosynthesis under different environmental conditions', *Progress in photosynthesis research*: Springer, pp. 221-224.

Bastidas, L. A., Gupta, H. V., Sorooshian, S., Shuttleworth, W. J. and Yang, Z. L. (1999) 'Sensitivity analysis of a land surface scheme using multicriteria methods', *Journal of Geophysical Research-Atmospheres*, 104(D16), pp. 19481-19490.

Best, M. J., Abramowitz, G., Johnson, H. R., Pitman, A. J., Balsamo, G., Boone, A., Cuntz, M., Decharme, B., Dirmeyer, P. A. and Dong, J. (2015) 'The plumbing of land surface models: benchmarking model performance', *Journal of Hydrometeorology*, 16, 1425-1442.

Cai, X., Yang, Z.-L., David, C. H., Niu, G.-Y., *and* Rodell, M. (2014a) 'Hydrological evaluation of the Noah-MP land surface model for the Mississippi River Basin', *Journal of Geophysical Research - Atmospheres*, 119, 23–38, doi:10.1002/2013JD020792.

Cai, X., Yang, Z.-L, Xia, Y., Huang, M., Wei, H., Leung, L.R., and Ek, M.B. (2014b) 'Assessment of simulated water balance from Noah, Noah-MP, CLM, and VIC over CONUS using the NLDAS test bed', *Journal of Geophysical Research-Atmospheres*, 119, 13,751-13,770, doi: 10.1002/2014JD022113.

Case, J. L., Kumar, S. V., Srikishen, J. and Jedlovec, G. J. (2011) 'Improving numerical weather predictions of summertime precipitation over the southeastern United States through a high-resolution initialization of the surface state', *Weather and Forecasting*, 26(6), pp. 785-807.

Chen, F. and Dudhia, J. (2001) 'Coupling an advanced land surface-hydrology model with the Penn State-NCAR MM5 modeling system. Part I: Model implementation and sensitivity', *Monthly Weather Review*, 129(4), pp. 569-585.

Chen, F., Janjić, Z. and Mitchell, K. (1997) 'Impact of atmospheric surface-layer parameterizations in the new land-surface scheme of the NCEP mesoscale Eta model', *Boundary-Layer Meteorology*, 85(3), pp. 391-421.

Chen, F., Mitchell, K., Schaake, J., Xue, Y. K., Pan, H. L., Koren, V., Duan, Q. Y., Ek, M. and Betts, A. (1996) 'Modeling of land surface evaporation by four schemes and comparison with FIFE observations', *Journal of Geophysical Research-Atmospheres*, 101(D3), pp. 7251-7268.

Collatz, G.J., Ball, J.T., Frivet, C., and Berry, J.A. (1991) 'Physiological and environmental regulation of stomatal conductance, photosynthesis and transpiration - a model that includes a laminar boundary layer'. *Agricultural and Forest Meteorology*, 52(2-4), pp. 107-136.

Cuntz, M., Mai, J., Samaniego, L., Clark, M., Wulfmeyer, V., Branch, O., Attinger, S., and Thober, S. (2016) 'The impact of standard and hard-coded parameters on the hydrologic fluxes in the Noah-MP land surface model, *Journal of Geophysical Research: Atmospheres.*, 121, 10,676–10,700, doi:10.1002/2016JD025097.

Dash, J. and Curran, P. J. (2004) 'The MERIS terrestrial chlorophyll index'. *International Journal of Remote Sensing*, 23, pp. 5403-5413.

Dee, D. P. (2005) 'Bias and data assimilation', *Quarterly Journal of the Royal Meteorological Society*, 131(613), pp. 3323-3344.

Demaria, E. M., Nijssen, B. and Wagener, T. (2007) 'Monte Carlo sensitivity analysis of land surface parameters using the Variable Infiltration Capacity model', *Journal of Geophysical Research: Atmospheres (1984–2012)*, 112(D11).

Deng, F., Chen, M., Plummer, S. and Pisek, J. (2006) 'Algorithm for global leaf area index retrieval using satellite imagery', *Geoscience and Remote Sensing, IEEE Transactions on*, 44(8), pp. 2219-2229.

Desai, A. R., Bolstad, P. V., Cook, B. D., Davis, K. J. and Carey, E. V. (2005) 'Comparing net ecosystem exchange of carbon dioxide between an old-growth and mature forest in the upper Midwest, USA', *Agricultural and Forest Meteorology*, 128(1), pp. 33-55.

Dickinson, R. E., Shaikh, M., Bryant, R., and Graumlich, L. (1998) 'Interactive canopies for a climate model', *Journal of Climate*, 11, pp. 2823-2836.

Didan, K. and Huete, A. (2006) 'MODIS vegetation index product series collection 5 change summary', *TBRS Lab, The University of Arizona*.

Ek, M. B., Mitchell, K. E., Lin, Y., Rogers, E., Grunmann, P., Koren, V., Gayno, G. and Tarpley, J. D. (2003) 'Implementation of Noah land surface model advances in the National Centers for Environmental Prediction operational mesoscale Eta model', *Journal of Geophysical Research-Atmospheres*, 108(D22), pp. 16.

468 Elbers, J. A., Jacobs, C. M., Kruijt, B., Jans, W. W. and Moors, E. J. (2011) 'Assessing the uncertainty of estimated annual
469 totals of net ecosystem productivity: A practical approach applied to a mid latitude temperate pine forest',
470 *Agricultural and forest meteorology*, 151(12), pp. 1823-1830.

471 Evensen, G. and van Leeuwen, P. J. (2000) 'An Ensemble Kalman Smoother for Nonlinear Dynamics', *Monthly Weather*
472 *Review*, 128(6), pp. 1852-1867.

473 Farquhar, G.D., von Caemmerer, S., and Berry, J.A. (1980) 'A biochemical model of photosynthetic CO_2 assimilation in
474 leaves of C3 species', *Planta*, 149, pp. 78-90.

475 Goldstein, A., Hultman, N., Fracheboud, J., Bauer, M., Panek, J., Xu, M., Qi, Y., Guenther, A. and Baugh, W. (2000) 'Effects
476 of climate variability on the carbon dioxide, water, and sensible heat fluxes above a ponderosa pine plantation in the
477 Sierra Nevada (CA)', *Agricultural and Forest Meteorology*, 101(2), pp. 113-129.

478 Gulden, L.E., and Yang, Z.-L. (2006) 'Development of species-based, regional emission capacities for simulation of biogenic
479 volatile organic compound emissions in land surce models: An example from Texas, USA', *Atmospheric*
480 *Environment*, 40, pp. 1464-1479.

481 Hanan, N., Boulain, N., Williams, C., Scholes, R. and Archibald, S. (2011) 'Functional convergence in ecosystem carbon
482 exchange in adjacent savanna vegetation types of the Kruger National Park, South Africa', *Ecosystem Function in*
483 *Savannas: Measurement and Modeling at Landscape to Global Scales. CRC Press, Boca Raton, USA*, pp. 7.

484 Hao, Z., AghaKouchak, A., Nakhjiri, N. and Farahmand, A. (2014) 'Global integrated drought monitoring and prediction
485 system', *Scientific Data*, 1.

486 Hogue, T. S., Bastidas, L., Gupta, H., Sorooshian, S., Mitchell, K. and Emmerich, W. (2005) 'Evaluation and transferability
487 of the Noah land surface model in semiarid environments', *Journal of Hydrometeorology*, 6(1), pp. 68-84.

488 Hogue, T. S., Bastidas, L. A., Gupta, H. V. and Sorooshian, S. (2006) 'Evaluating model performance and parameter behavior
489 for varying levels of land surface model complexity', *Water resources research*, 42(8).

490 Hou, T., Zhu, Y., Lü, H., Sudicky, E., Yu, Z. and Ouyang, F. (2015) 'Parameter sensitivity analysis and optimization of Noah
491 land surface model with field measurements from Huaihe River Basin, China', *Stochastic Environmental Research*
492 *and Risk Assessment*, 29(5), pp. 1-19.

493 Hou, Z., Huang, M., Leung, L. R., Lin, G. and Ricciuto, D. M. (2012) 'Sensitivity of surface flux simulations to hydrologic
494 parameters based on an uncertainty quantification framework applied to the Community Land Model', *Journal of*
495 *Geophysical Research: Atmospheres (1984–2012)*, 117(D15).

496 Huete, A. R. (1988) 'A soil-adjusted vegetation index (SAVI)', *Remote Sensing of Environment*, 25(3), pp. 295-309.

497 Jasechko, S., Sharp, Z. D., Gibson, J. J., Birks, S. J., Yi, Y. and Fawcett, P. J. (2013) 'Terrestrial water fluxes dominated by
498 transpiration', *Nature*, 496(7445), pp. 347-350.

499 Jiang, Z., Huete, A. R., Didan, K. and Miura, T. (2008) 'Development of a two-band enhanced vegetation index without a
500 blue band', *Remote Sensing of Environment*, 112(10), pp. 3833-3845.

501 Jordan, R. (1991) *A one-dimensional temperature model for a snow cover: Technical documentation for SNTHERM. 89*:
502 DTIC Document.

503 Koren, V., Schaake, J., Mitchell, K., Duan, Q. Y., Chen, F. and Baker, J. M. (1999) 'A parameterization of snowpack and
504 frozen ground intended for NCEP weather and climate models', *Journal of Geophysical Research: Atmospheres*
505 *(1984–2012)*, 104(D16), pp. 19569-19585.

Kumar, S. V., Peters-Lidard, C. D., Santanello, J. A., Reichle, R. H., Draper, C. S., Koster, R. D., Nearing, G. S. and Jasinski, M. F. (2015) 'Evaluating the utility of satellite soil moisture retrievals over irrigated areas and the ability of land data assimilation methods to correct for unmodeled processes', *Hydrology and Earth Systems Science*, 19, 4463-4478.

Kumar, S. V., Reichle, R. H., Harrison, K. W., Peters‐Lidard, C. D., Yatheendradas, S. and Santanello, J. A. (2012) 'A comparison of methods for a priori bias correction in soil moisture data assimilation', *Water Resources Research*, 48(3).

Liang, X., Wood, E. F. and Lettenmaier, D. P. (1996) 'Surface soil moisture parameterization of the VIC-2L model: Evaluation and modification', *Global and Planetary Change*, 13(1), pp. 195-206.

Mendoza, P. A., Clark, M. P., Barlage, M., Rajagopalan, B., Samaniego, L., Abramowitz, G. and Gupta, H. (2015) 'Are we unnecessarily constraining the agility of complex process‐based models?', *Water Resources Research*, 51(1), pp. 716-728.

Miller, D. A. and White, R. A. (1998) 'A conterminous United States multilayer soil characteristics dataset for regional climate and hydrology modeling', *Earth interactions*, 2(2), pp. 1-26.

Niu, G.-Y. and Yang, Z.-L. (2006) 'Effects of frozen soil on snowmelt runoff and soil water storage at a continental scale', *Journal of Hydrometeorology*, 7(5), pp. 937-952.

Niu, G. Y. and Yang, Z. L. (2004) 'Effects of vegetation canopy processes on snow surface energy and mass balances', *Journal of Geophysical Research: Atmospheres (1984–2012)*, 109(D23).

Niu, G. Y., Yang, Z. L., Dickinson, R. E. and Gulden, L. E. (2005) 'A simple TOPMODEL‐based runoff parameterization (SIMTOP) for use in global climate models', *Journal of Geophysical Research: Atmospheres (1984–2012)*, 110(D21).

Niu, G. Y., Yang, Z. L., Dickinson, R. E., Gulden, L. E. and Su, H. (2007) 'Development of a simple groundwater model for use in climate models and evaluation with Gravity Recovery and Climate Experiment data', *Journal of Geophysical Research: Atmospheres (1984–2012)*, 112(D7).

Niu, G. Y., Yang, Z. L., Mitchell, K. E., Chen, F., Ek, M. B., Barlage, M., Kumar, A., Manning, K., Niyogi, D. and Rosero, E. (2011) 'The community Noah land surface model with multiparameterization options (Noah‐MP): 1. Model description and evaluation with local‐scale measurements', *Journal of Geophysical Research: Atmospheres (1984–2012)*, 116(D12).

Oleson, K. W., Lawrence, D. M., Gordon, B., Flanner, M. G., Kluzek, E., Peter, J., Levis, S., Swenson, S. C., Thornton, E. and Feddema, J. (2010) 'Technical description of version 4.0 of the Community Land Model (CLM)'.

Pielke, R. A., Lee, T. J., Copeland, J. H., Eastman, J. L., Ziegler, C. L. and Finley, C. A. (1997) 'Use of USGS-provided data to improve weather and climate simulations', *Ecological Applications*, 7(1), pp. 3-21.

Pitman, A. J. T. (1994) 'Assessing the sensitivity of a land-surface scheme to the parameter values using a single column model', *Journal of Climate*, 7(12), pp. 1856-1869.

Reichle, R. H. (2008) 'Data assimilation methods in the Earth sciences', *Advances in Water Resources*, 31(11), pp. 1411-1418, doi: http://dx.doi.org/10.1016/j.advwatres.2008.01.001.

Reichle, R. H. and Koster, R. D. (2004) 'Bias reduction in short records of satellite soil moisture', *Geophysical Research Letters*, 31(19).

Rodell, M., Houser, P. R., Jambor, U. e. a., Gottschalck, J., Mitchell, K., Meng, C. J., Arsenault, K., Cosgrove, B., Radakovich, J. and Bosilovich, M. (2004) 'The global land data assimilation system', *Bulletin of the American Meteorological Society*, 85(3), pp. 381-394.

Rosero, E., Yang, Z. L., Wagener, T., Gulden, L. E., Yatheendradas, S. and Niu, G. Y. (2010) 'Quantifying parameter sensitivity, interaction, and transferability in hydrologically enhanced versions of the Noah land surface model over transition zones during the warm season', *Journal of Geophysical Research: Atmospheres (1984–2012)*, 115(D3).

Rosolem, R., Gupta, H. V., Shuttleworth, W. J., Gonçalves, L. G. G. and Zeng, X. (2013) 'Towards a comprehensive approach to parameter estimation in land surface parameterization schemes', *Hydrological Processes*, 27(14), pp. 2075-2097.

Running, S. W., Nemani, R. R., Heinsch, F. A., Zhao, M., Reeves, M. and Hashimoto, H. (2004) 'A continuous satellite-derived measure of global terrestrial primary production', *Bioscience*, 54(6), pp. 547-560.

Saltelli, A., Chan, K. and Scott, E. M. (2009) *Sensitivity Analysis.* Chichester, NY: Wiley.

Schaake, J. C., Koren, V. I., Duan, Q.-Y., Mitchell, K. and Chen, F. (1996) 'Simple water balance model for estimating runoff at different spatial and temporal scales', *Journal of Geophysical Research - Atmospheres*, 101, pp. 7461-7475.

Suni, T., Rinne, J., Reissell, A., Altimir, N., Keronen, P., Rannik, U., Maso, M., Kulmala, M. and Vesala, T. (2003) 'Long-term measurements of surface fluxes above a Scots pine forest in Hyytiala, southern Finland, 1996-2001', *Boreal Environment Research*, 8(4), pp. 287-302.

Veenendaal, E. M., Kolle, O. and Lloyd, J. (2004) 'Seasonal variation in energy fluxes and carbon dioxide exchange for a broad‐leaved semi‐arid savanna (Mopane woodland) in Southern Africa', *Global Change Biology*, 10(3), pp. 318-328.

Verseghy, D. L. (1991) 'CLASS—A Canadian land surface scheme for GCMs. I. Soil model', *International Journal of Climatology*, 11(2), pp. 111-133.

Vogelmann, J. E., Howard, S. M., Yang, L., Larson, C. R., Wylie, B. K. and Van Driel, N. (2001) 'Completion of the 1990s National Land Cover Data Set for the conterminous United States from Landsat Thematic Mapper data and ancillary data sources', *Photogrammetric Engineering and Remote Sensing*, 67(6).

Xia, Y., Ek, M., Wood, E., Sheffield, J., Luo, L. and Mo, K. (2011) 'North American Land Data Assimilation System (NLDAS) in support of the U.S. drought and flood analysis, monitoring, and prediction, including National Integrated Drought Information System (NIDIS)'. *International Union of Geodesy and Geophysics*, Melbourne, Australia.

Xue, Y., Sellers, P. J., Kinter, J. L. and Shukla, J. (1991) 'A simplified biosphere model for global climate studies', *Journal of Climate*, 4(3), pp. 345-364.

Xue, Y., Zeng, F. J. and Schlosser, C. A. (1996) 'SSiB and its sensitivity to soil properties—A case study using HAPEX-Mobilhy data', *Global and Planetary Change*, 13(1), pp. 183-194.

Yang, Z.-L. and Dickinson, R. E. (1996) 'Description of the Biosphere-Atmosphere Transfer Scheme (BATS) for the Soil Moisture Workshop and evaluation of its performance', *Global and Planetary Change*, 13(1), pp. 117-134.

Yang, Z.-L., Dickinson, R. E., Robock, A. and Vinnikov, K. Y. (1997) 'Validation of the snow submodel of the biosphere-atmosphere transfer scheme with Russian snow cover and meteorological observational data', *Journal of climate*, 10(2), pp. 353-373.

Yang, Z.-L., Niu, G.-Y., Mitchell, K. E., Chen, *F.*, Ek, M. B., Barlage, *M.*, Longuevergne,*L.*, Manning,*K.*, Niyogi, *D.*, Tewari, *M.*, *and* Xia, Y. (2011) 'The community Noah land surface model with multiparameterization options (Noah-MP): 2. Evaluation over global river basins', Journal of Geophysical Research, 116, *D12110*, *doi:*10.1029/2010JD015140.

Zhu, Z., Bi, J., Pan, Y., Ganguly, S., Anav, A., Xu, L., Samanta, A., Piao, S., Nemani, R. R. and Myneni, R. B. (2013) 'Global data sets of vegetation leaf area index (LAI) 3g and Fraction of Photosynthetically Active Radiation (FPAR) 3g derived from Global Inventory Modeling and Mapping Studies (GIMMS) Normalized Difference Vegetation Index (NDVI3g) for the period 1981 to 2011', *Remote Sensing*, 5(2), pp. 927-948.

Tables

Table 1: FluxNet sites and data-years used in this study.

						Depth[a]	
Name	**Country**	**Lat**	**Lon**	**Plant Type**	**Years**	**SM1**	**SM2**
Amplero	Italy	41.90°N	13.61°E	Grassland	2003, 2004, 2006	5 cm	10 cm
Blodgett	United States	38.90°N	120.63°W	Evergreen Needleleaf	2000, 2001, 2002, 2003, 2004, 2005	10 cm	30 cm
El Saler	Spain	39.25°N	0.32°W	Evergreen Needleleaf	1999, 2000, 2002, 2003	surficial[b]	medium[b]
El Saler (2)	Spain	39.28°N	0.32°W	Cropland	2006	surficial[b]	medium[b]
Fort Peck	United States	48.31°N	105.10°W	Grassland	2003, 2004, 2005	10 cm	30 cm
Hyytiala	Finland	61.85°N	24.29°E	Evergreen Needleleaf	2001, 2004	2-3 cm	5 cm
Kruger	South Africa	25.02°S	31.50°E	Savanna	2002, 2003	3 cm	7 cm
Loobos	Netherlands	52.17°N	5.74°W	Evergreen Needleleaf	1999, 2003, 2004, 2005, 2006	3 cm	20 cm
Mopane	Botswana	19.92°S	23.56°E	Woody Savanna	2000, 2001	10 cm	50 cm
Sylvania	United States	46.24°N	89.35°W	Mixed Forest	2002, 2003, 2004, 2005	5 cm	10 cm

[a] Depth from surface of soil moisture measurements

[b] Soil moisture depths at the two El Saler sites are given as *surficial*, *medium* and *deep*. We treat the surficial moisture measurement as corresponding to the top modeled layer, and the medium measurement as corresponding to the second modeled layer. The justification for this is that we are only concerned here with the variation in the model response, not with the absolute difference between model response and measurement.

Table 2: Noah-MP parameterization options. For more information see Niu et al. (2011).

Physical Process	Available Options	Option(s) Used
Vegetation	1. Prescribed LAI and shade fraction 2. LAI and shade fraction calculated from dynamic simulation of carbon uptake and partitioning 3. Shade fraction calculated from prescribed LAI 4. Prescribed LAI and constant shade fraction	1. Prescribed LAI and shade fraction 2. Dynamic simulation
Stomatal resistance	1. Ball-Berry (Ball et al., 1987) 2. Jarvis (Chen et al., 1996)	1. Ball-Berry (required for dynamic vegetation) 2. Jarvis (only for vegetation option 1)
Soil moisture factor for stomatal resistance	1. Noah-type (based on soil moisture) (Chen et al., 1996)) 2. CLM-type (based on stomatal resistance) (Oleson et al., 2010) 3. SSiB-type (based on stomatal resistance) (Xue et al., 1991)	1. Noah-type (for vegetation options 1 and 2) 2. CLM-type (only for vegetation option 2) 3. SSiB-type (only for vegetation option 2)
Runoff & groundwater	1. SIMGM: based on TOPMODEL (Niu et al., 2007) 2. SIMTOP: SIMGM with an equilibrium water table and zero-flux lower boundary (Niu et al., 2005) 3. Infiltration-excess surface runoff and free drainage (Schaake et al., 1996) 4. BATS runoff and free drainage (Yang and Dickinson, 1996)	1. SIMGM
Surface layer drag coefficient	1. Monin-Obukhov 2. Noah-type (Chen et al., 1997)	1. Monin-Obukhov
Super-cooled liquid water	1. Standard freezing point depression (Niu and Yang, 2006) 2. Variant of standard (Koren et al., 1999)	1. Standard
Frozen soil permeability	1. Uses total soil moisture to compute hydraulic properties (Niu and Yang, 2006) 2. Uses only liquid water content to compute hydraulic properties (Koren et al., 1999)	1. Total soil moisture
Radiation transfer	1. Modified two-stream scheme (Niu and Yang, 2004) 2. Two-stream with a 3D canopy structure 3. Two-stream with canopy gap equal to 1-(shade fraction)	2. Two-stream with a 3D canopy structure
Snow albedo	1. BATS (considers variations in snow age, grain size growth, and impurity) (Yang et al., 1997) 2. CLASS (only considers overall snow age) (Verseghy, 1991)	2. CLASS
Frozen/liquid partitioning	1. Based on Jordan (1991) 2. Based on the offset threshold: $T_{air} < T_{frz} + 2.2K$ where T_{frz} is a constant 3. Based on the threshold: $T_{air} < T_{frz}$	1. Based on Jordan (1991)

Table 3: Noah-MP parameters for dynamic vegetation that are considered in this study. Parameters that dominate sensitivity are in bold italics.

Parameter Name	Description	Units	Min Value	Max Value
	Vegetation Parameters			
Z0MVT	***Momentum roughness length***	***[m]***	***0.06***	***1.10***
HVT	***Height of top of canopy***	***[m]***	$max\left(1, \frac{1}{2} \times \alpha\right)$[a]	$min(20, 2 \times \alpha)$[a]
HVB	Height of bottom of canopy	[m]	0.1×HVT	0.9×HVT
RC	Tree crown radius	[m]	0.08	3.60
RHOL-vis	Leaf reflectance in visible spectrum	[~]	0	0.11
RHOL-nir	Leaf reflectance in NIR	[~]	0	0.58
RHOS-vis	Stem reflectance in visible spectrum	[~]	0	0.36
RHOS-nir	Stem reflectance in NIR	[~]	0	0.58
TAUL-vis	Leaf transmittance in visible spectrum	[~]	0	0.07
TAUL-nir	Leaf transmittance in NIR	[~]	0	0.25
TAUS-vis	Stem transmittance in visible spectrum	[~]	0	0.22
TAUS-nir	Stem transmittance in NIR	[~]	0	0.38
XL	Leaf/stem orientation index	[~]	-0.30	0.25
LTOVRC	***Leaf and stem/organic turnover rate***	***[1/s]***	***0***	***1.2***
DILEFC	Coefficient for leaf stress death related to carbon	[1/s]	0	1.8
DILEFW	***Coefficient for leaf stress death related to water***	***[1/s]***	***0***	***4***
RMF25	***Leaf maintenance respiration at 25℃***	***[μmol/m²s]***	***0***	***4***
SLA	***Single-side leaf area per Kg***	***[m²/kg]***	***10***	***80***
FRAGR	Fraction of growth respiration	[~]	0	0.2
TMIN	Minimum temperature for photosynthesis	[K]	0	273
VCMX25	***Maximum rate of carboxylation at 25℃***	***[μmol/m²s]***	***0***	***80***
TDLEF	Characteristic temperature for leaf freezing	[K]	268	278
BP	Minimum leaf conductance	[μmol/m^{2}s]	2000	10^{14}
MP	Slope of conductance-to-photosynthesis relationship	[~]	6	9
QE25	***Quantum efficiency at 25℃***	***[μmol/m²s]***	***0***	***0.6***
RMS25	Stem maintenance respiration at 25℃	[μmol/m^{2}s]	0	0.9
RMR25	Root maintenance respiration at 25℃	[μmol/m^{2}s]	0	0.36
FOLNMX	Baseline foliage nitrogen concentration	[%]	0	1.5
WRRAT	Wood to non-wood ratio	[~]	0	30
MRP	Microbial respiration parameter	[μmol/kg s]	0	0.37
	Soil Parameters			
CSOIL	Volumetric soil heat capacity	[J/m^{3}K]	2x10^6	3x10^6
BEXP	***Pore size distribution index***	***[~]***	***4.26***	***11.55***
DKSAT	***Saturated soil hydraulic conductivity***	***[m/s]***	***1x10^{-6}***	***1.4x10^{-5}***
DWSAT	Saturated soil hydraulic diffusivity	[m^2/s]	5x10^{-6}	1.4x10^{-5}
PSISAT	Saturated soil matric potential	[m/m]	0.036	0.468
QUARTZ	Soil quartz content	[m^3/m^3]	0.25	0.82
SMCDRY	Soil moisture where direct evaporation stops	[m^3/m^3]	0.01	0.12
SMCMAX	***Porosity***	***[m³/m³]***	***0.40***	***0.70***[b]
SMCREF	***Field capacity***	***[m³/m³]***	$\frac{1}{3} \times$***SMCMAX***	***SMCMAX***[c]
SMCWLT	***Wilting point soil moisture***	***[m³/m³]***	***SMCDRY***	***SMCREF***[c]
ZBOT	Depth to deep soil temperature	[m]	2	4
TBOT	Deep soil temperature	[K]	274	300

[a] The α parameter in the vegetation height parameter sampling ranges represents the default top-of-canopy vegetation height in the Noah-MP parameter tables for the specific vegetation class. These values range from 1 m to 20 m, and the vegetation classes are listed in Table 1.

[b] Maximum porosity in the STATSGO-FAO soil table is 0.468, which is too low to capture the dynamic range of many soils, so we extended the range of this variable to 0.70 [m^3/m^3].

[c] These soil parameters were calculated from a hyperparameter that represented the percentage of the difference between the listed lower bound and the parameter listed as the upper bound. All sensitivity indices related to this parameter actually refer to the sensitivity of the hyperparameter. This was done to ensure that certain parameters did not exceed their dynamic ranges, as defined by other parameters that were allowed to vary.

Table 4: Noah-MP parameters for prescribed LAI that are considered in this study. Parameters that dominate sensitivity are in bold italics.

Parameter Name	Description	Units	Min Value	Max Value
	Vegetation Parameters			
Z0MVT	***Momentum roughness length***	***[m]***	***0.06***	***1.10***
HVT	***Height of top of canopy***	***[m]***	$\boldsymbol{max\left(1,\frac{1}{2}\times\alpha\right)}$[a]	$\boldsymbol{min(20,2\times\alpha)}$[a]
HVB	Height of bottom of canopy	[m]	0.1×HVT	0.9×HVT
RC	Tree crown radius	[m]	0.08	3.60
RHOL-vis	Leaf reflectance in visible spectrum	[~]	0	0.11
RHOL-nir	***Leaf reflectance in NIR***	***[~]***	***0***	***0.58***
RHOS-vis	Stem reflectance in visible spectrum	[~]	0	0.36
RHOS-nir	Stem reflectance in NIR	[~]	0	0.58
TAUL-vis	Leaf transmittance in visible spectrum	[~]	0	0.07
TAUL-nir	Leaf transmittance in NIR	[~]	0	0.25
TAUS-vis	Stem transmittance in visible spectrum	[~]	0	0.22
TAUS-nir	Stem transmittance in NIR	[~]	0	0.38
HS	***Vapor pressure deficit parameter***	***[~]***	***36.25***	***1000***
TOPT	***Optimum transpiration air temperature***	***[K]***	***272***	***310***
RGL	***Radiation stress parameter***	***[~]***	***30***	***1000***
RSMAX	Maximum stomatal resistance	[m]	2000	5000
RSMIN	***Minimum stomatal resistance***	***[m]***	***40***	***400***
LAI[b]	***Leaf area index multiplier***	***[m^2/m^2]***	***0***	***5***
SAI[b]	***Stem area index multiplier***	***[m^2/m^2]***	***0***	***5***
	Soil Parameters			
CSOIL	Volumetric soil heat capacity	[J/m^3K]	$2x10^6$	$3x10^6$
BEXP	***Pore size distribution index***	***[~]***	***4.26***	***11.55***
DKSAT	***Saturated soil hydraulic conductivity***	***[m/s]***	***$1x10^{-6}$***	***$1.4x10^{-5}$***
DWSAT	Saturated soil hydraulic diffusivity	[m^2/s]	$5x10^{-6}$	$1.4x10^{-5}$
PSISAT	Saturated soil matric potential	[m/m]	0.036	0.468
QUARTZ	Soil quartz content	[m^3/m^3]	0.25	0.82
SMCDRY	Soil moisture where direct evaporation stops	[m^3/m^3]	0.01	0.12
SMCMAX	***Porosity***	***[m^3/m^3]***	***0.40***	***0.70***[c]
SMCREF	***Field capacity***	***[m^3/m^3]***	$\frac{1}{3}\times$***SMCMAX***	***SMCMAX***[d]
SMCWLT	***Wilting point soil moisture***	***[m^3/m^3]***	***SMCDRY***	***SMCREF***[d]
ZBOT	Depth to deep soil temperature	[m]	2	4
TBOT	Deep soil temperature	[K]	274	300

[a] The α parameter in the vegetation height parameter sampling ranges represents the default top-of-canopy vegetation height in the Noah-MP parameter tables for the specific vegetation class. These values range from 1 m to 20 m, and the vegetation classes are listed in Table 1.

[b] LAI and SAI are prescribed to the model as monthly time series, and we calculated sensitivity to time series multipliers instead of directly on the actual twelve LAI (SAI) values.

[c] These parameters were calculated from a hyperparameter that represented the percentage of the difference between the listed lower bound and the parameter listed as the upper bound. All sensitivity indices related to this parameter actually refer to the sensitivity of the hyperparameter. This was done to ensure that certain parameters did not exceed their dynamic ranges, as defined by other parameters that were allowed to vary.

[d] Maximum porosity in the STATSGO-FAO soil table is 0.468, which is too low to capture the dynamic range of many soils, so we extended the range of this variable to 0.70 [m^3/m^3].

Figures

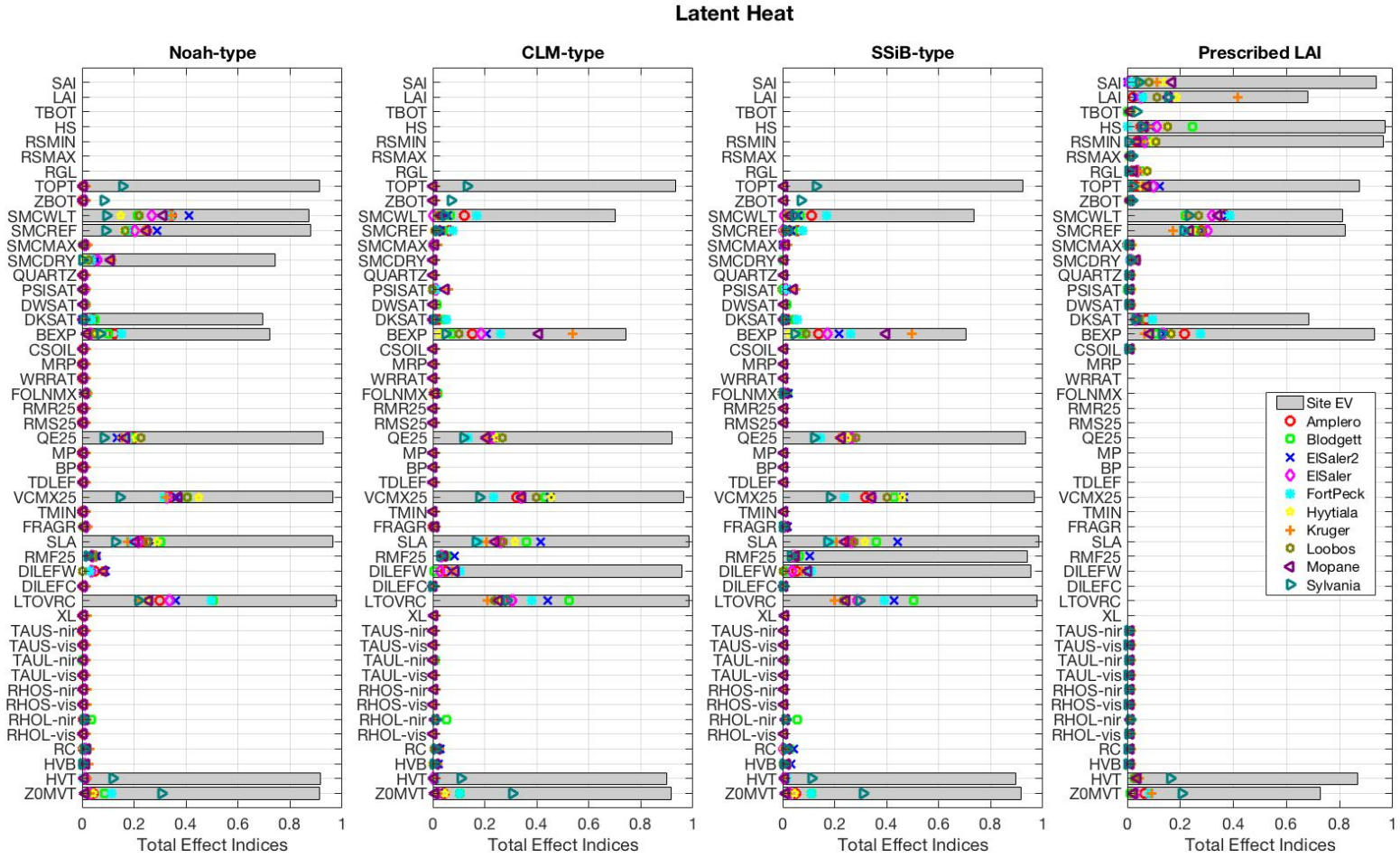

Figure 1: Average total effect indices for latent heat flux over all the years of data at each FluxNet site. Different parameters were assessed for the three configurations of Noah-MP using dynamic vegetation versus the one configuration with static vegetation. Gray bars show the fraction of variance in the total sensitivity indices explained by site-by-site differences (EV = fraction of explained variance), whereas the remaining fraction of variance is due to inter-annual differences at individual sites.

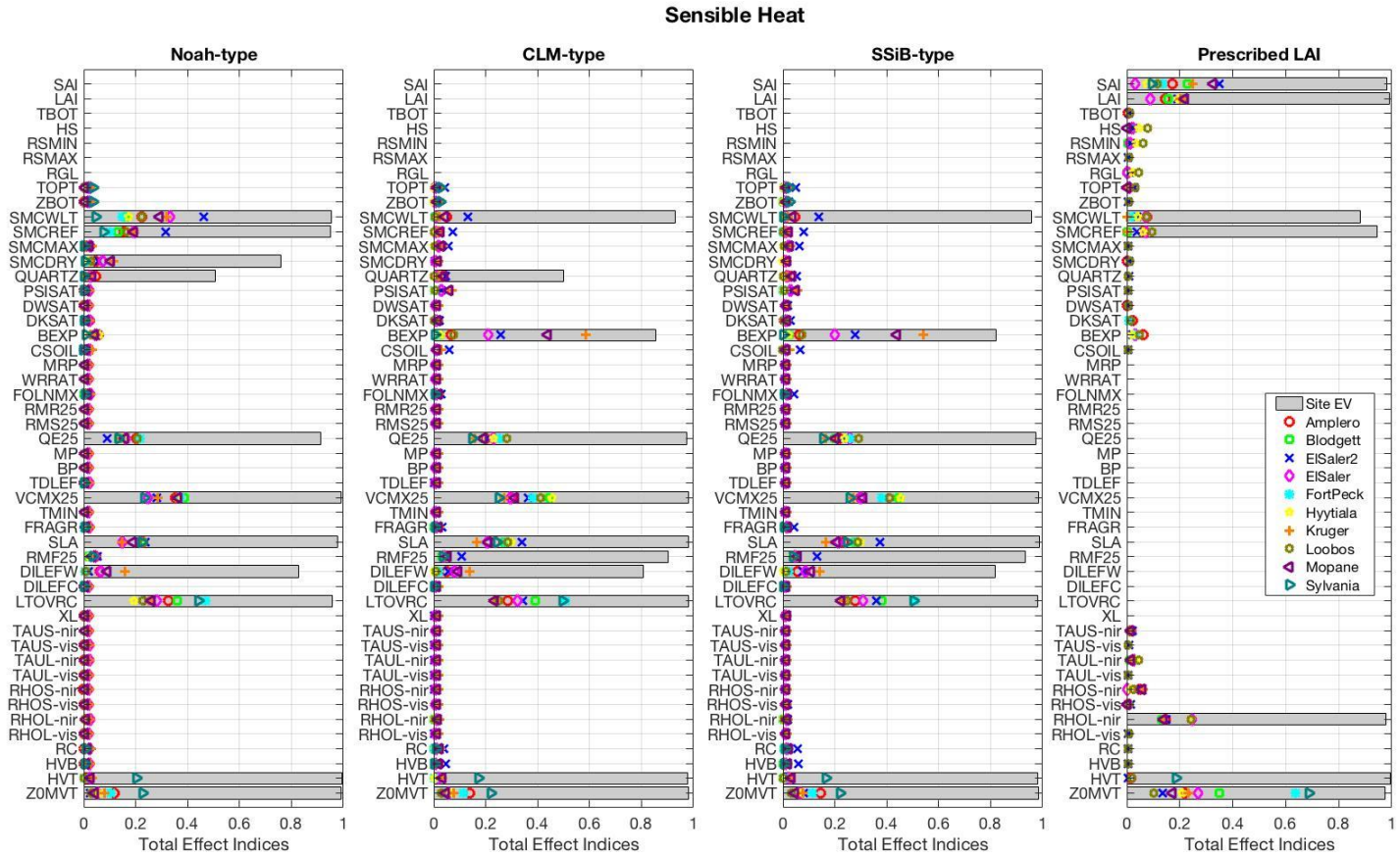

634

635 **Figure 2:** Same as Figure 1 except for sensible heat flux.

636

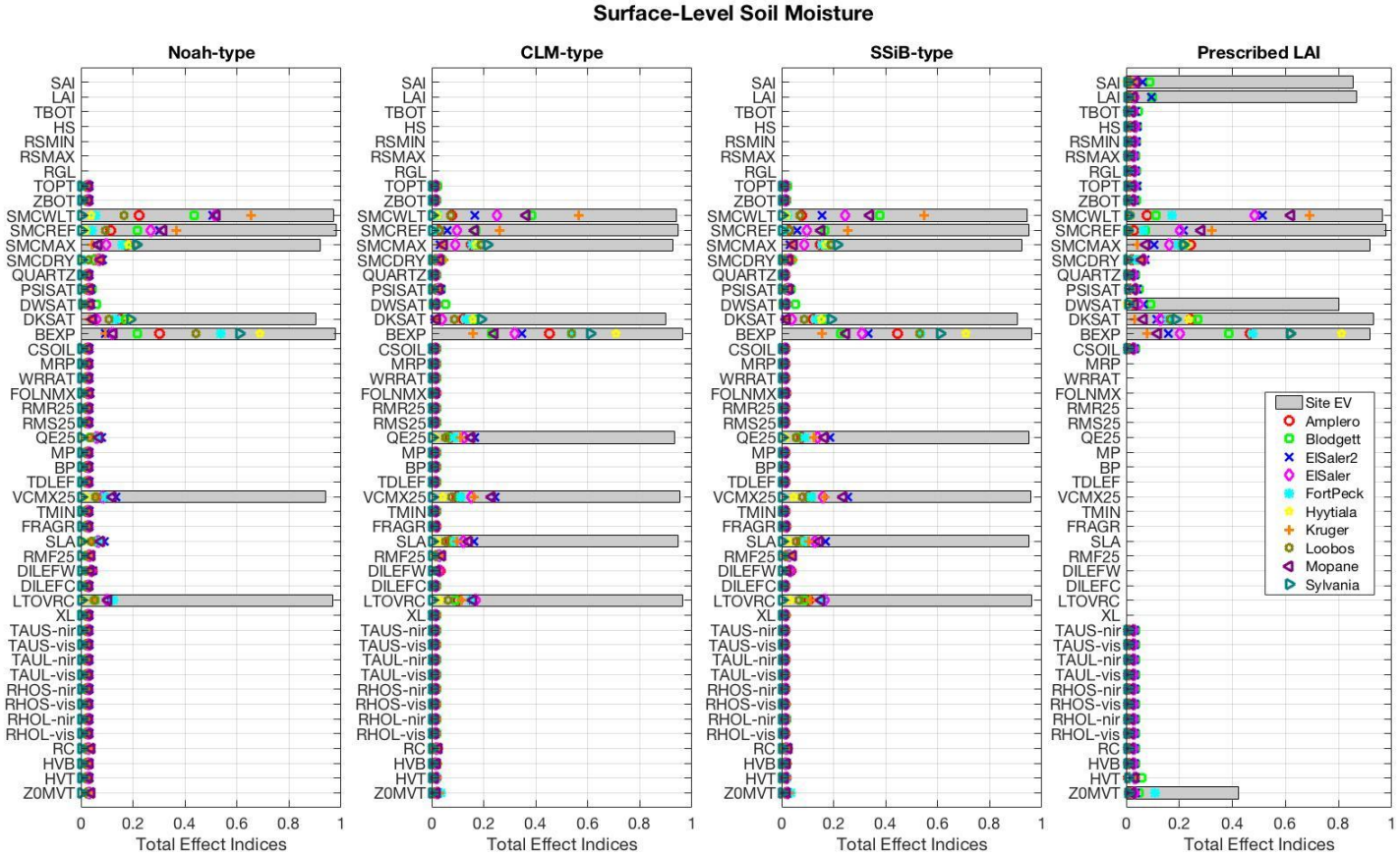

637

638 **Figure 3:** Same as Figure 1 except for top-layer soil moisture.

639

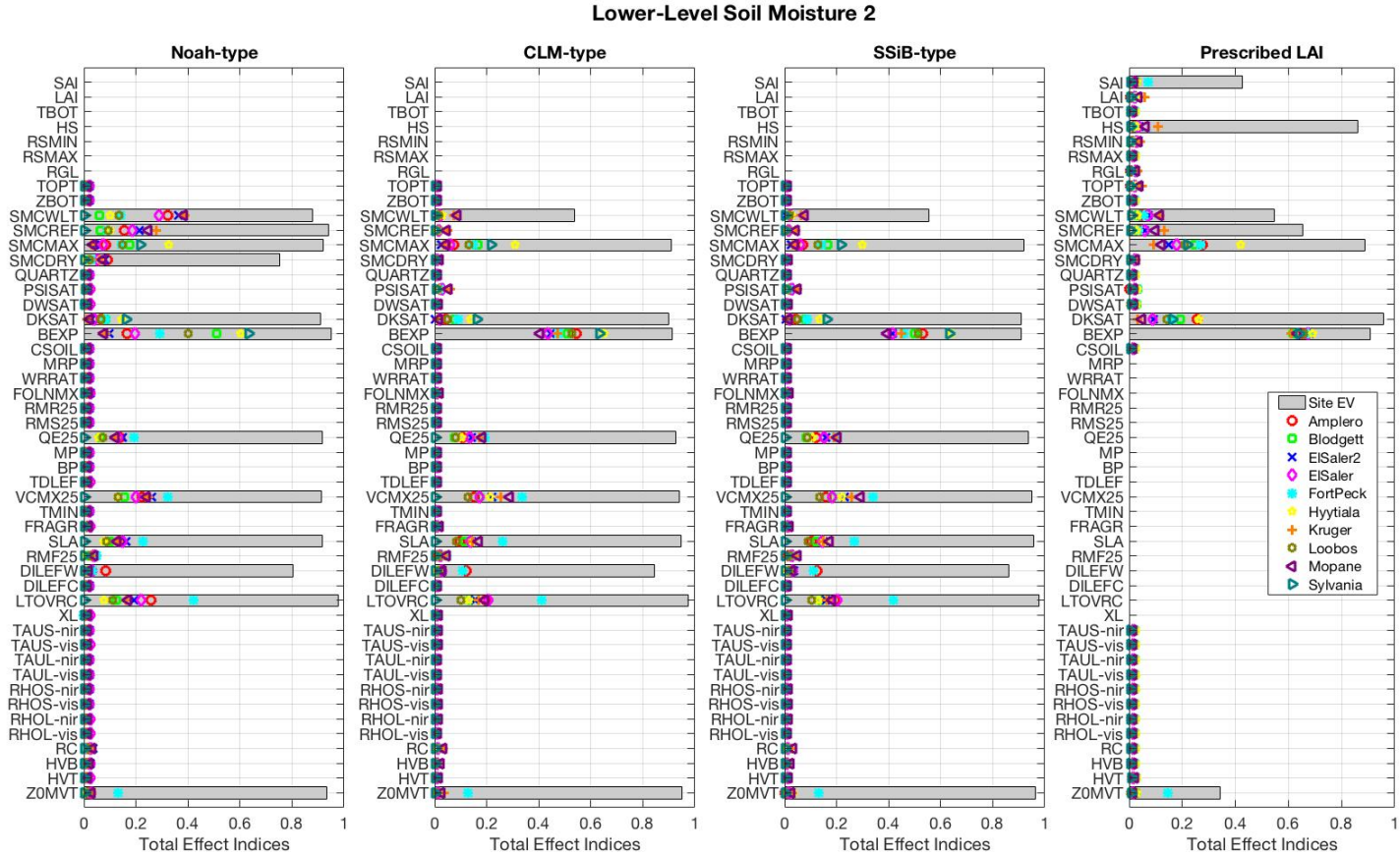

640

641 **Figure 4:** Same as Figure 1 except for second-layer soil moisture.

642

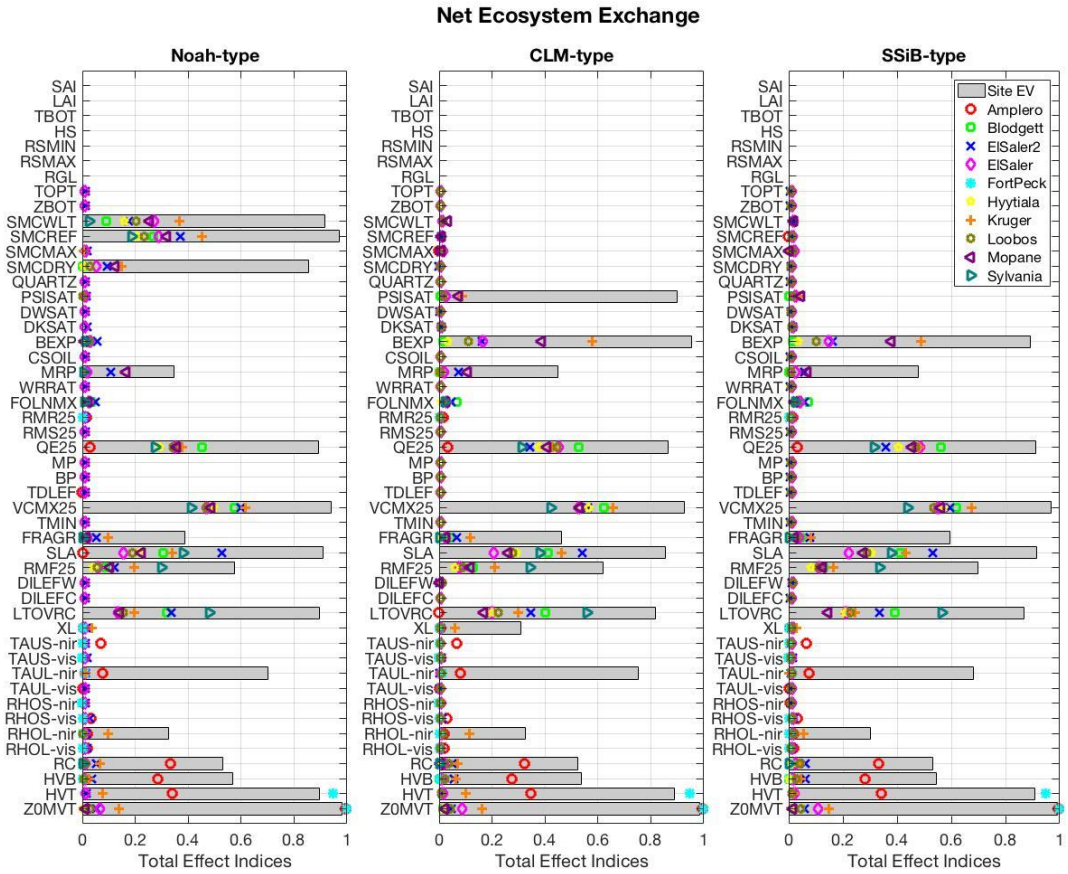

643
644 **Figure 5:** Same as Figure 1 except for net ecosystem exchange (NEE). The static-vegetation configuration of Noah-MP does not
645 simulate NEE.